



HAL
open science

On the impact of topography and building mask on time varying gravity due to local hydrology

Sabrina Deville, Thomas Jacob, Jean Chery, Cedric Champollion

► To cite this version:

Sabrina Deville, Thomas Jacob, Jean Chery, Cedric Champollion. On the impact of topography and building mask on time varying gravity due to local hydrology. *Geophysical Journal International*, 2013, 192 (1), pp.82-93. 10.1093/gji/ggs007 . hal-00795590

HAL Id: hal-00795590

<https://hal.science/hal-00795590>

Submitted on 26 Mar 2021

HAL is a multi-disciplinary open access archive for the deposit and dissemination of scientific research documents, whether they are published or not. The documents may come from teaching and research institutions in France or abroad, or from public or private research centers.

L'archive ouverte pluridisciplinaire **HAL**, est destinée au dépôt et à la diffusion de documents scientifiques de niveau recherche, publiés ou non, émanant des établissements d'enseignement et de recherche français ou étrangers, des laboratoires publics ou privés.

On the impact of topography and building mask on time varying gravity due to local hydrology

S. Deville,¹ T. Jacob,² J. Chéry¹ and C. Champollion¹

¹Laboratoire Géosciences Montpellier, Université Montpellier 2, 34090 Montpellier, France. E-mail: deville@gm.univ-montp2.fr

²Bureau de recherches Géologiques et Minières, 45060 Orléans, France

Accepted 2012 October 3. Received 2012 April 11; in original form 2012 October 3

SUMMARY

We use 3 yr of surface absolute gravity measurements at three sites on the Larzac plateau (France) to quantify the changes induced by topography and the building on gravity time-series, with respect to an idealized infinite slab approximation. Indeed, local topography and buildings housing ground-based gravity measurement have an effect on the distribution of water storage changes, therefore affecting the associated gravity signal. We first calculate the effects of surrounding topography and building dimensions on the gravity attraction for a uniform layer of water. We show that a gravimetric interpretation of water storage change using an infinite slab, the so-called Bouguer approximation, is generally not suitable. We propose to split the time varying gravity signal in two parts (1) a surface component including topographic and building effects (2) a deep component associated to underground water transfer. A reservoir modelling scheme is herein presented to remove the local site effects and to invert for the effective hydrological properties of the unsaturated zone. We show that effective time constants associated to water transfer vary greatly from site to site. We propose that our modelling scheme can be used to correct for the local site effects on gravity at any site presenting a departure from a flat topography. Depending on sites, the corrected signal can exceed measured values by 5–15 μGal , corresponding to 120–380 mm of water using the Bouguer slab formula. Our approach only requires the knowledge of daily precipitation corrected for evapotranspiration. Therefore, it can be a useful tool to correct any kind of gravimetric time-series data.

Key words: Time variable gravity; Hydrology; Site effects.

1 INTRODUCTION

Water storage changes have a direct influence on the time-variable gravity at the Earth's surface through Newtonian attraction (e.g. Lambert & Beaumont 1977). Repeating ground-based gravity measurements allows for a direct monitoring of the temporal variations of water storage (e.g. Harnisch & Harnisch 2006; Van Camp *et al.* 2006; Jacob *et al.* 2008). A notable feature of gravity measurements is that they integrate water storage changes at a mesoscale within a radius some hundreds of meters around the measurement site (Hokkanen *et al.* 2006; Van Camp *et al.* 2006; Creutzfeldt *et al.* 2008; Hasan *et al.* 2008; Naujoks *et al.* 2010a), within all possible water stores: snow, surface waters, soil, unsaturated and saturated zones.

Because gravity declines as the inverse of the squared distance for a given mass unit, the immediate surroundings of gravity measurement sites hence play a key role in the gravity response due to water storage changes (Creutzfeldt *et al.* 2008, 2010b). Local topography has an influence on the distribution of water relative to the gravity meter, which, in turn, influences the gravity response.

For example, underground measurement sites record a gravity decrease after rainfall events (Van Camp *et al.* 2006; Longuevergne *et al.* 2009; Lampitelli & Francis 2010), because the additional water masses are for a large part above the gravity meter. Accounting for these effects needs an accurate representation of the topography and some knowledge of how infiltration occurs.

Buildings housing measurement sites may also alter the distribution of water storage change, by acting as impervious layers effectively precluding rainfall from directly infiltrating beneath the instrument. This effect has been rarely investigated and has been called 'umbrella' effect by Creutzfeldt *et al.* (2010b). These authors point out that these effects are site dependent, and that they may lead to underestimate water storage changes from gravity measurements.

We follow this idea and attempt to quantify, using a reservoir model, how water storage changes and local site effects affect the gravity measurements performed on a karst system during 3 yr (Jacob *et al.* 2008). These authors compared the absolute gravity (AG) time-series at three measurement sites to the mean area water storage changes at the karst system scale using the Bouguer slab approximation. Differences between the sites were interpreted as

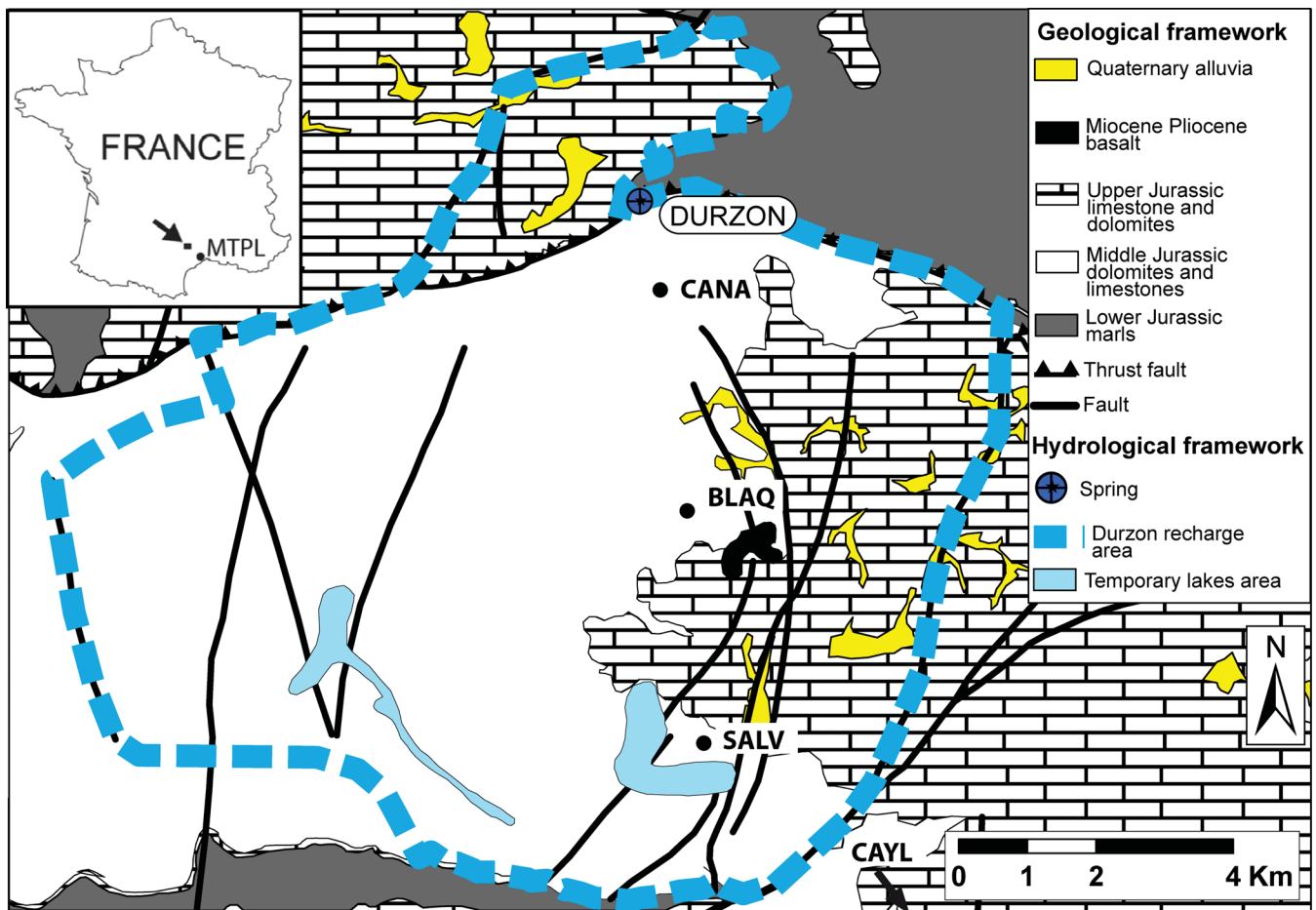


Figure 1. Hydrogeological location map of the studied area, modified after (Ricard & Bakalowicz 1996). Gravimetric sites CANA, BLAQ and SALV are indicated by black dots. MTPL refers to Montpellier city.

due to the spatial heterogeneity of water storage, which was further evidenced in Jacob *et al.* (2010). In these previous studies, the site effects corresponding to the local topography and to the building mask effect were not accounted for. Also, no local hydrological modelling was performed to extract meaningful information about water storage dynamics at each site. In this study, we consider these effects and attempt to separate the hydrological part of the signal from the site effect. We evaluate the *a priori* local site effects on gravity at each measurement site by a forward computing approach. We propose a reservoir modelling scheme taking into account local site effects. We finally discuss how our modelling allows obtaining gravity measurements independent of local site effects.

2 DESCRIPTION OF THE MEASUREMENT SITES

AG measurements were performed at three sites on the Durzon karst system in the Grand Causses area, southern French Massif Central: La Salvetat (called SALV hereafter), La Blaquererie (BLAQ) and Les Canalettes (CANA) which are at decreasing distance of the Durzon spring (Fig. 1). Each site was measured on a concrete pillar and measurement position is at 1.2 m above this pillar.

SALV site is the most distant from the spring (Fig. 2), and gravity measurements are done at the centre of a building of 500 m² in area at this site. An underground tank captures rainfall nearly at the same

elevation as that of the gravimeter, beneath the building. Elevation around the building varies between 800 and 820 m with a maximum gradient on NE–SW section (Fig. 2). The gravimetric site is located in the vicinity of a temporary lakes area. Chert marl covers the temporary lake area. In the Northern part of SALV site, an outcrop of Upper Jurassic limestone is visible (Fig. 2b).

BLAQ site is located in the middle part of Durzon karst system. There, gravity is monitored in a 10 m² shack. Elevation around the hut varies between 840 m at the South and 826 m at the North of the site (Fig. 3).

The last site (CANA) site is located in the northern part of the system, where gravity measurements are performed in the Eastern part of a building 150 m² in area (Fig. 4). A tank stores runoff water from the roof and is at the same elevation as the gravimeter (Fig. 4b). Elevation around the building varies between 725 and 760 m. It can be separated in two parts: the northwestern part with higher elevations and the southeastern part with a flatter topography at lower elevations. An important elevation variation lies at the north of building, with a cliff reaching some 10 m in height (Figs 4a and b).

3 OBSERVATIONS AND DATA PROCESSING

AG measurements were performed from January 2006 to October 2008 at a monthly frequency at three sites: CANA, BLAQ and

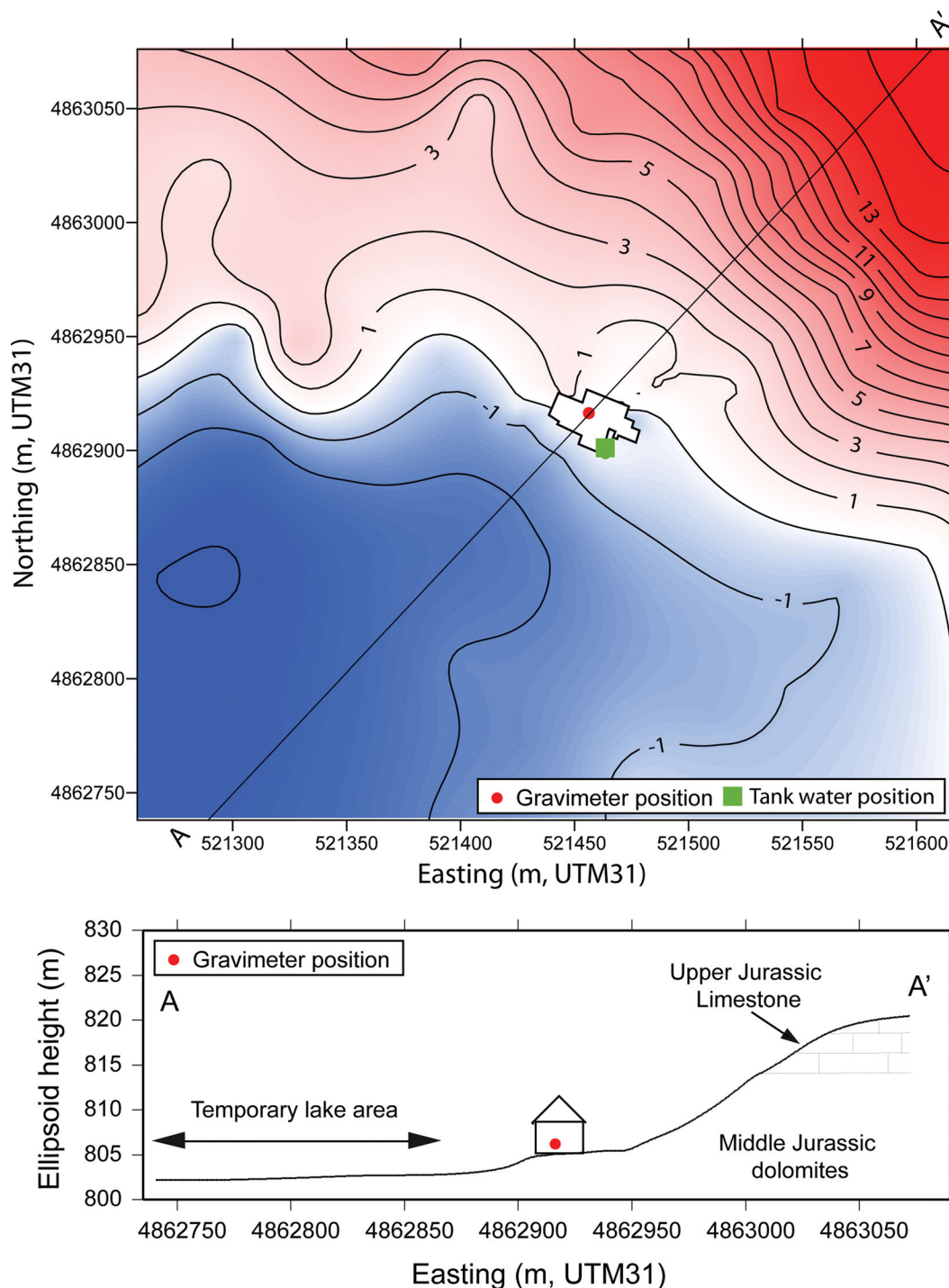


Figure 2. (a) Topography around SALV and ground plan of the building. Gravimeter position and water tank position are shown; (b) cross-section of the studied area with the main characteristics of the site. Note the proximity of temporary lakes area.

SALV (Fig. 5a). The absolute gravimeter (FG5#228) was mostly used to measure gravity (FG5#206 was used to measure the three sites once at November 2006). A comparison of two FG5 reveals that the gravity value differs by less than $1 \mu\text{Gal}$ between them (Le Moigne, personal communication). The mean value of g is estimated from a series of 100 drops every hours (set) and the mean AG value is calculated by averaging several sets (>12 sets). The overall systematic instrumental uncertainty is of $1.9 \mu\text{Gal}$ (Niebauer *et al.* 1995). Raw data are processed using a protocol described by

Jacob *et al.* (2008) that is not detailed here. The global contribution of hydrology is computed using GLDAS/NOAH (Rodell *et al.* 2004) model of soil moisture, snow and canopy water content variations as a 0.25° grid. The global gravimetric effect including both attraction and deformation is estimated following the method of Boy *et al.* (1998) and is removed from gravity time-series. The maximum global gravimetric effect in the studied area reaches $\pm 2 \mu\text{Gal}$ and the amplitudes of ECMWF and GLDAS models differ by less than $0.5 \mu\text{Gal}$ (Jacob *et al.* 2008). By removing this global contribution

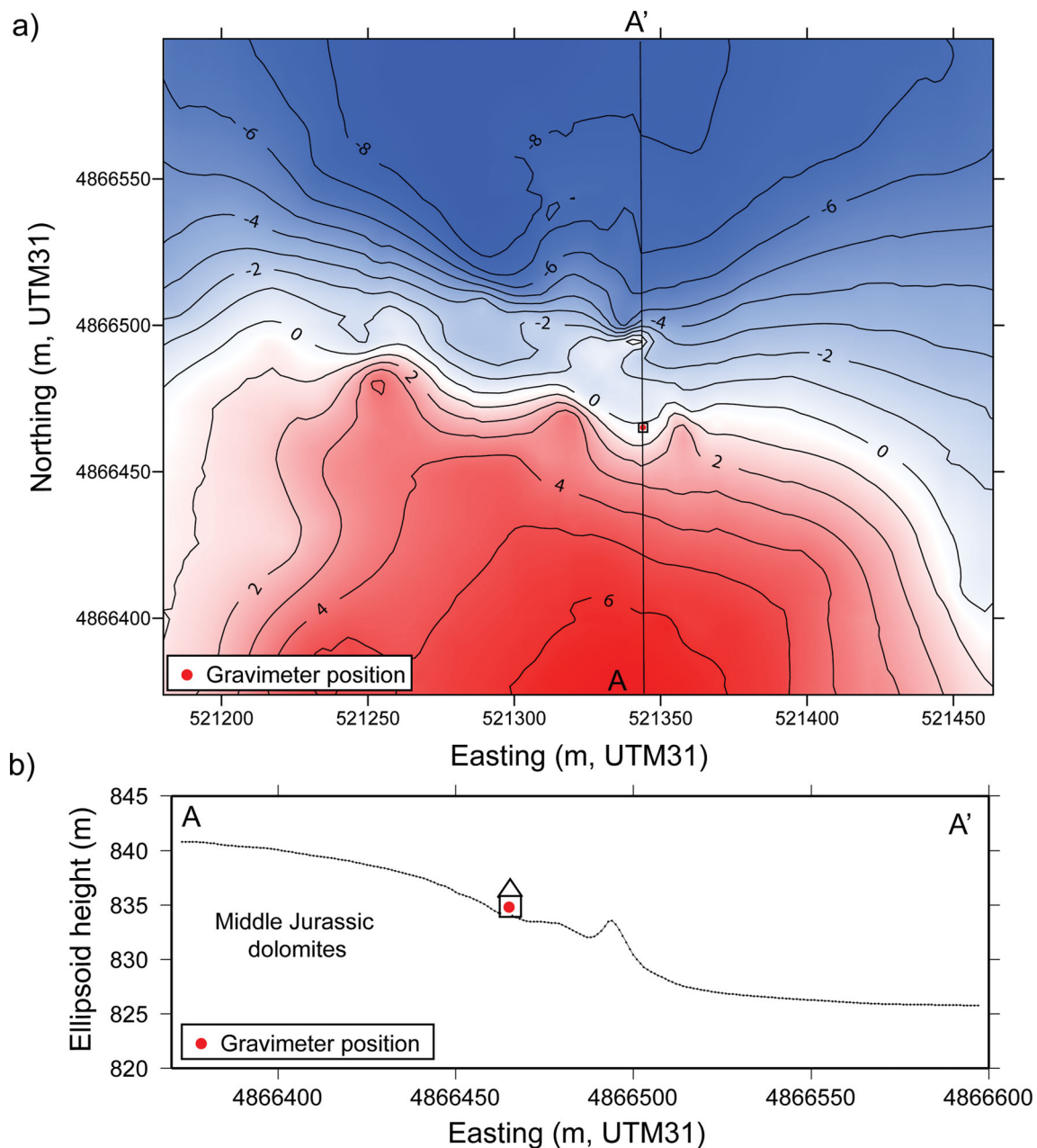


Figure 3. (a) Topography around BLAQ site and ground plan of the building; (b) cross-section of the studied area with the main characteristics of the site.

from the time-series, we assume that the residual gravity time-series represent the signature of local hydrologic processes. This residual signal will be used in the forthcoming modelling.

Tipping bucket rain gauges have been installed at the AG sites between 2006 and 2009. Annual precipitation is comparable at the three sites (Table 1) with a difference of less than 10 per cent except for the year 2009 during which the rain gauges at SALV malfunctioned. In the following, we use rainfall data from BLAQ site as input for our models. Daily potential evapotranspiration (PET) is calculated using Penman-Monteith's formula by Météo-France at Caylar station (7 km to the SE of SALV site) provided by Météo-France and we assume that the estimate is valid for the Durzon karst system. To obtain daily actual evapotranspiration (AET), a scaling factor (k) must be applied to the PET. The comparison between yearly total AET, yearly total PET and mass balance modelling at

the Durzon scale (Jacob 2009) yields a scaling factor between 0.5 and 0.8. Keeping in mind that precise yearly value of scaling factor cannot be determined on the base on existing data, we apply a scaling factor of 0.65 to the daily PET to obtain the daily AET (Fig. 5c). The scaling factor is comparable to a crop coefficient, yet it does not evolve seasonally as a result of the stage of development of plants (Allen *et al.* 1998) and the water availability in the soil. Another solution would have been to invert for the crop coefficient by including it in our modelling scheme (Seibert 2005) or to simulate the value of AET (Zhang *et al.* 2011), but that would have increased the number of model parameters and their associate uncertainty.

Precipitation on the Larzac plateau are highest during autumn and winter (Fig. 5b). Because AET is smallest during these months, most of the winter precipitation infiltrates into the ground. The gravity

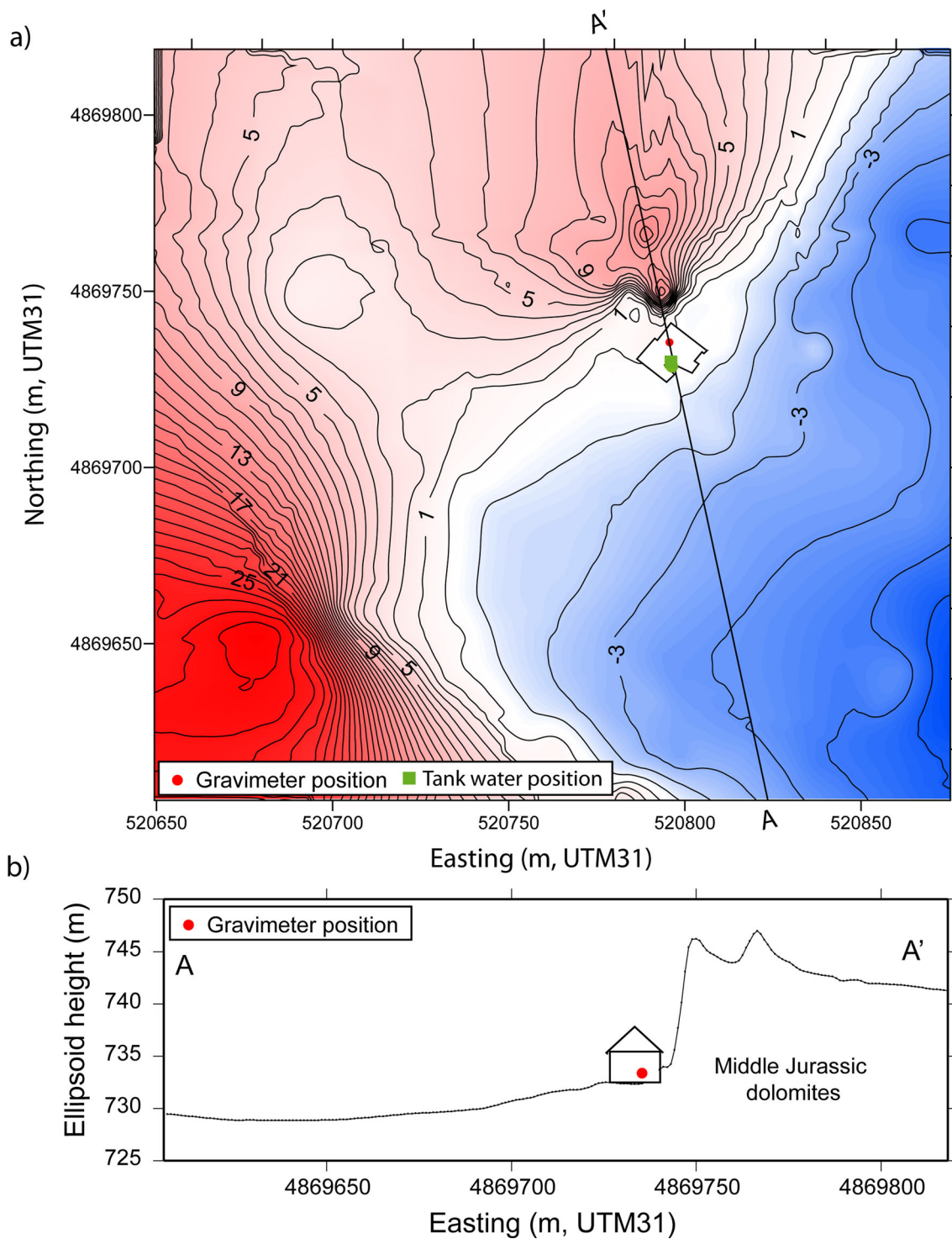


Figure 4. (a) Topography around CANA site and ground plan of the building. Gravimeter position and water tank position are shown; (b) cross-section of the studied area with the main characteristics of the site.

therefore increases during the weeks following precipitations events such as in 2006 January, 2006 October and 2007 November to 2008 January (Figs 5a and b). During the dry season (May to September), gravity decreases at every site. We arbitrarily set the first gravity value to zero for each site. The significant differences between the time-series (Fig. 5a) may be linked to differences in local water storage dynamics at each site, as invoked by Jacob *et al.* (2008), but also to differences in local site effects.

4 DIRECT ESTIMATION OF LOCAL SITE EFFECTS

In the following, we examine the effects of surrounding topography and building dimensions on the gravity attraction for a uniform layer of water. In an ideal case, where topography is flat, rainfall and hydrological parameters of the underground homogeneous and the effect of the building negligible, the gravity change Δg from

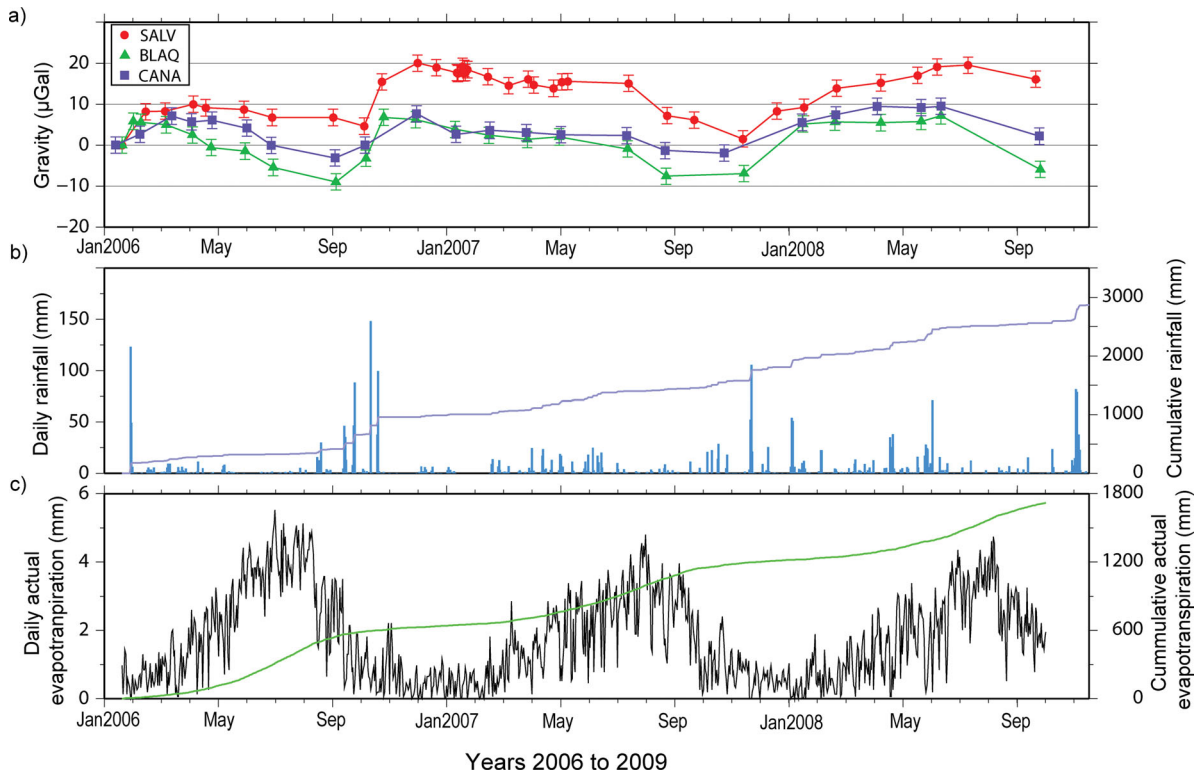


Figure 5. (a) Absolute gravity measurements at SALV, CANA and BLAQ sites. Error bars represent measurements uncertainty; (b) daily and cumulative rainfall and (c) daily and cumulative actual evapotranspiration.

Table 1. Annual cumulative rainfall in mm at BLAQ, SALV and CANA site for the years 2007, 2008, 2009.

Site	2007	2008	2009
BLAQ	811	1034	875
SALV	768	1067	759
CANA	808	1080	—

water height changes Δh may be computed using the formula for an infinite slab:

$$\Delta g = 2\pi\rho G\Delta h \quad (1)$$

known as Bouguer's formula, where G is universal gravitational constant and ρ is the water density. However, local geometric effects influence the spatial distribution of water and its attraction, such as the topography in the surroundings of the gravity sites, the area of the measurement building and the position of the gravimeter within it (Fig. 6). For example, a local topography where the surface is above the gravity measurement site leads to a negative gravity value if water storage occurs at shallow depth. Also, a building partially masks the effect of rainfall, as its roof precludes water from directly infiltrating beneath the gravimeter. Snow on a roof can also influence gravity measurements (Mäkinen & Tattari 1988). Finally, the spatial heterogeneity of hydrological parameters such as porosity and permeability modifies water content distribution. These parameters are spatially heterogeneous and are mostly unknown for the studied sites.

To evaluate the impact of building and topography on measured gravity at 1.2 m above the ground, we compute the attraction of water right on the surface at each site. A digital elevation model (DEM) encompassing terrain 300 m around each site was built using kinematic GPS (accuracy of 0.1 m). We also use spirit levelling at

building vicinity (vertical accuracy of respectively 0.05 m). Our DEM resolution ranges from 0.2 m in the near field to 2 m in the far field). The shape of each building is introduced in the DEM and corresponds to a “no-rain” zone for the evaluation of local site effects hereafter. Runoff water from the roofs is stored in partially open tanks at nearly the same elevation as that of the gravimeter, whose gravity impact is computed to be weak ($<1 \mu\text{Gal}$). The stored water is depleted by evaporation and also used to irrigate nearby crops. The gravity attraction of surface water for each site is computed using a point mass equation for a given unit of rain. Because the distance between the site measurement and the land topography is larger than 2 m, the error due to the point mass approximation versus the attraction of equivalent prism is smaller than $1 \mu\text{Gal}$.

The resulting gravity attraction is compared to the one provided by an infinite slab (Bouguer approximation). For each site, a ratio C is defined as the ratio between the real site attraction and the infinite slab attraction associated to a uniform precipitation on a flat surface. In the presence of a flat topography and no building, to the ratio C would be equal to unity. Effects of both surrounding topography and of the building are detailed in Table 2. C_{topo} is calculated without the gap induced by the building and corresponds to the topographic effect only. A value close to 1 indicates that topography can be approximated as a flat surface beneath the gravimeter with no significant effects on gravity. To estimate the umbrella effect of the building C_{building} , we compute the effect of a rain layer that exactly matches the building shape. A value close to 1 of C_{building} indicates that the building gap has an important effect on gravity value. The total effect of the topography and building umbrella effect is given by C_{total} , which corresponds to the difference between C_{topo} and C_{building} . Values of 0.53, -0.06 and 0.12 are found for C_{total} at BLAQ, CANA and SALV sites, respectively, when no infiltration

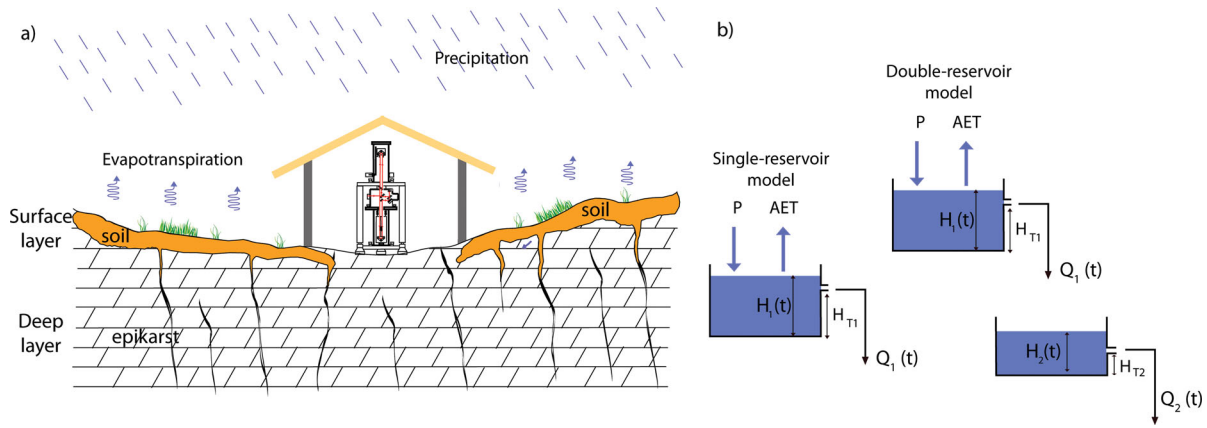


Figure 6. (a) Schematic representation of water storage and transfer around a building between the surface layer (soil) and the epikarstic zone below (b) tank models used for simulation (see Section 5).

Table 2. Values of C coefficient at BLAQ, CANA and SALV sites for different depths. This coefficient is the ratio between the actual site attraction and the infinite slab attraction (see Section 4). For each site, column 1 refers to the topographic effect (C_{topo}), column 2 refers to the building effect ($C_{building}$), and column 3 refers to the whole local site effect only (C_{total}) that is equal to $C_{topo} - C_{building}$. Building areas are given in parenthesis.

Depth (m)	BLAQ (10 m ²)			CANA (150 m ²)			SALV (500 m ²)		
	C_{topo}	$C_{building}$	C_{total}	C_{topo}	$C_{building}$	C_{total}	C_{topo}	$C_{building}$	C_{total}
0	0.87	0.34	0.53	0.66	0.72	-0.06	0.98	0.86	0.12
0.5	0.88	0.23	0.65	0.72	0.65	0.07	0.98	0.82	0.16
1	0.88	0.17	0.71	0.77	0.61	0.16	0.98	0.78	0.20
2	0.9	0.1	0.80	0.82	0.49	0.33	0.97	0.71	0.26

has occurred, that is, when water is distributed on the topography. C_{topo} at CANA site has a smaller value than for the two other sites. High terrain elevation above the gravimeter position in its direct vicinity causes the negative value of C_{total} for CANA site (Fig. 4). For SALV and BLAQ, elevation variations are equally distributed around the gravimeter elevation and C_{topo} are close to 1. On the other hand $C_{building}$ is much greater at SALV than at BLAQ, because of the smaller building size of BLAQ, which leads to a smaller umbrella effect. As a result, the ratio C_{total} is lower at SALV than at BLAQ site. These computations point out the importance of local effects on gravity signal such as described in other studies (e.g. Naujoks *et al.* 2010a; Creutzfeldt *et al.* 2010c).

In the field, both vertical and horizontal water transfer occur when rainwater infiltrates (Fig. 6a). Horizontal infiltration beneath a building reduces the umbrella effect. Forward modelling of rainwater infiltration would make an estimation of local site effects possible. This would however require detailed knowledge of the 3-D hydraulic properties of the underground, which are unknown and very difficult to estimate in karst systems. We assume that water infiltration occurs vertically, acknowledging that it is a gross simplification of infiltration process. For this reason, we limit our computation to a depth of infiltration of 2 m. Because water masses eventually infiltrate below the gravity site position, the coefficient C_{topo} increases with infiltration depth (Table 2). In contrast, the local site effect of the building ($C_{building}$) gradually decreases relative to the surrounding masses, as infiltration depth increases. The combination of these two effects leads C_{total} to significantly increase when infiltration depth reaches 2 m. In conclusion, the above calculations show that gravity changes associated to water storage changes at the three sites cannot be simulated using an infinite slab approximation. Local site effects must be taken into account if one wants to interpret time varying gravity in term of hydrological processes.

5 WATER TRANSFER AND LOCAL SITE EFFECT MODELLING

5.1 Model description

In this section, we present a reservoir modelling scheme that accounts for local site effects while inverting for parameters of reservoir models. We adapt here a reservoir modelling strategy to simulate water storage changes (Fleury *et al.* 2007). Reservoir outflow is governed by effective water height in each reservoir and their characteristic discharge constants. We recall that these heights do not correspond to physical water heights as water is distributed across the unsaturated zone. Rather, they can be associated to an integrated value of saturation change in the site's vicinity. For the sake of testing models of increasing complexity, we consider a single and a two-reservoir model (Fig. 6b), which both contain a surface reservoir intercepting rainfall minus AET. Output flow Q_1 from reservoir 1 at the surface occurs when the water level $h_1(t)$ is higher than a threshold H_1 , according to a linear discharge law (Maillet 1905) defined by a characteristic transfer time T_1 . H_1 represents here the soil capacity before discharge. Output flow Q_2 of the reservoir 2 at depth occurs in the same way that for the reservoir when the water level $h_2(t)$ is higher than a threshold H_2 .

$$Q_1(t) = \frac{1}{T_1 (h_1(t) - H_1)} \quad (2)$$

$$Q_2(t) = \frac{1}{T_2 (h_2(t) - H_2)} \quad (3)$$

In the two-reservoir model, a deep reservoir captures discharge water from the surface reservoir, and its water level $h_2(t)$ decreases through a linear flow law controlled by a characteristic transfer time T_2 . Because the deep reservoir is not affected by evapotranspiration

Table 3. Best adjusted model parameters and rms for single and two-reservoir models at BLAQ, CANA and SALV sites. Parameter uncertainties are associated to the best simulations (see text for explanation). C_1 and C_2 correspond to the scaling coefficients associated to the upper and the lower reservoirs, T_1 and T_2 is the characteristic transfer time for the upper and the lower reservoirs, and H_1 is the threshold height of the upper reservoir.

	BLAQ		CANA		SALV	
	Single reservoir	Two reservoirs	Single reservoir	Two reservoirs	Single reservoir	Two reservoirs
C_1	0.85 ± 0.06	0.70 ± 0.10	0.43 ± 0.07	0.29 ± 0.09	0.73 ± 0.11	0.19 ± 0.14
H_1 (mm)	82 ± 51	173 ± 47	51 ± 101	297 ± 32	21 ± 46	129 ± 39
T_1 (d)	147 ± 41	68 ± 51	391 ± 82	38 ± 12	237 ± 63	27 ± 10
C_2	-	1.24 ± 0.42	-	0.94 ± 0.21	-	1.24 ± 0.15
T_2 (d)	-	46 ± 75	-	174 ± 101	-	259 ± 39
rms (μGal)	1.28	1.23	1.87	1.55	3.1	2.089

process, water level cannot decrease below H_2 . Therefore, the dynamic evolution of the model does not depend on H_2 , which is set to 0. The single and two-reservoir models yield water levels $h_1(t)$ and $h_2(t)$, respectively, which are computed by the time integration of flow rate equations.

The water levels are converted into gravity attraction using the infinite slab approximation, scaled by a factor accounting for local site effects. Thus, the simulated gravity change can be expressed as

$$g_{\text{sim}}(t) = 2\pi G\rho_w [C_1 h_1(t) + C_2 h_2(t)], \quad (4)$$

where C_1 and C_2 are site dependent scaling coefficients associated to the upper and the lower reservoirs, respectively. The gravity time-series at each site (Fig. 5a) are used to calibrate the model parameters: initial water heights in the reservoirs, discharge constants (T_1 , T_2), threshold of the surface reservoir (H_1), and scaling factors relative to local site effects (C_1 , C_2). The objective function is the rms between observed and simulated gravity. Single and double reservoir models allow testing the effect of increasing model complexity on fit performance. For an equivalent RMS, the model having the fewest parameters is chosen as most adequate. A simple stochastic inversion with a total of 50 000 random sampling in the parameter space is performed. The uncertainty of the estimated parameters is explored using a perturbation approach (Wagener *et al.* 2004). We search all parameter sets for which the rms does not increase beyond 10 per cent of its optimal value. Using this criterion, we calculate parameter uncertainties displayed in Table 3.

5.2 Results

At BLAQ site, there is no significant difference in rms between single and two-reservoir model (Table 3), which means that the single reservoir model is adequate in representing the gravity variations. The estimated value of C_1 is close to unity. The characteristic transfer time is of about five months.

At CANA site, a small but significant decrease in rms (Table 3) indicates that the two-reservoir model is more adequate than the single reservoir model in explaining gravity changes. For the two-reservoir model, the value of C_1 parameter is 0.29. The value of C_2 relative to water in the deeper reservoir is close to unity. A characteristic transfer time of one month between surface and depth reservoir is found.

At SALV site, a large rms reduction is observed between single and two-reservoir models, with the two-reservoir model yielding the smallest rms. For this model, the value of the C_1 parameter is 0.19, which is slightly higher than that obtained at CANA site. The value of the C_2 parameter is 1.24, clearly greater than unity. The characteristic transfer time from the surface reservoir to the deep

one is short (27 d). The characteristic transfer time of the deep tank is about 1 yr (259 d).

The time-series of water heights from the model allows comparing modelled and measured gravity values. Modelled water heights at SALV site are represented in Fig. 7(b) for the two-reservoir model. The step-like influence of rainfall on the surface reservoir water level is clearly apparent, yet it is not so on the gravity time-series (Fig. 7a), because of the low value of C_1 . Rather, gravity seems to be influenced by the water level changes in the deep reservoir, in which the high-frequency content of precipitation has effectively been filtered out. Modelled water heights at CANA site show larger water storage variation in the surface reservoir than the deep reservoir (Fig. 8b). However, C_1 coefficient has a value of 0.29 and C_2 coefficient is close to unity. According to eq. (4), this implies that gravity changes are influenced by deeper water height variations rather than surface water height variations. Estimated water heights at BLAQ site (Fig. 9b) and corresponding gravity (Fig. 9a) for the single reservoir model account well the observed gravity, in which the step-like influence of rainfall is clearly visible.

For CANA and SALV sites, for which the two-reservoir model seems more adequate, deep reservoir parameter dispersion is always greater than that of the surface reservoir (Table 3). This may be the consequence of the uncertainty of the water input to the deep reservoir, which is a modelled quantity. Therefore, more trade-offs in the parameter space occur, that is, the uncertainty of the input value to the deep reservoir is greater than the uncertainty of the measured input value to the surface reservoir provided by precipitation and AET. Furthermore, the number and frequency of gravity measurements seem to have a direct influence on the dispersion of parameters of the surface reservoir. It can readily be observed for the discharge constants, whose dispersions are much greater at CANA ($T_2 = 174 \pm 101$ d) than at SALV ($T_2 = 259 \pm 39$ d) sites (Table 3), possibly due to a higher gravity sampling at the latter site (Fig. 5a). Also, gravity measurements shortly after rainfall are particular lacking at CANA site. A higher measurement rate (provided for example by a superconducting gravimeter) should improve both the value and the uncertainty of some estimated parameters. This would specially apply to the determination of T_1 for sites CANA and SALV. Due to an average measurement rate of one month on these sites, estimated values of T_1 at CANA and SALV (respectively 38 and 27 d) are likely higher bounds of the real time transfer values.

Another source of parameter estimation problem could be tied to evapotranspiration. Among input data, AET is the most uncertain data that we have included in the model. To test the sensitivity of the model with respect to the factor k , we run the model for values of k ranging from 0.5 to 0.8. Parameter values of each site obtained with different values of k moderately alter the result of simulations. As an example, the characteristic time T_2 of the site CANA displays values of 260, 259 and 164 d when k values are

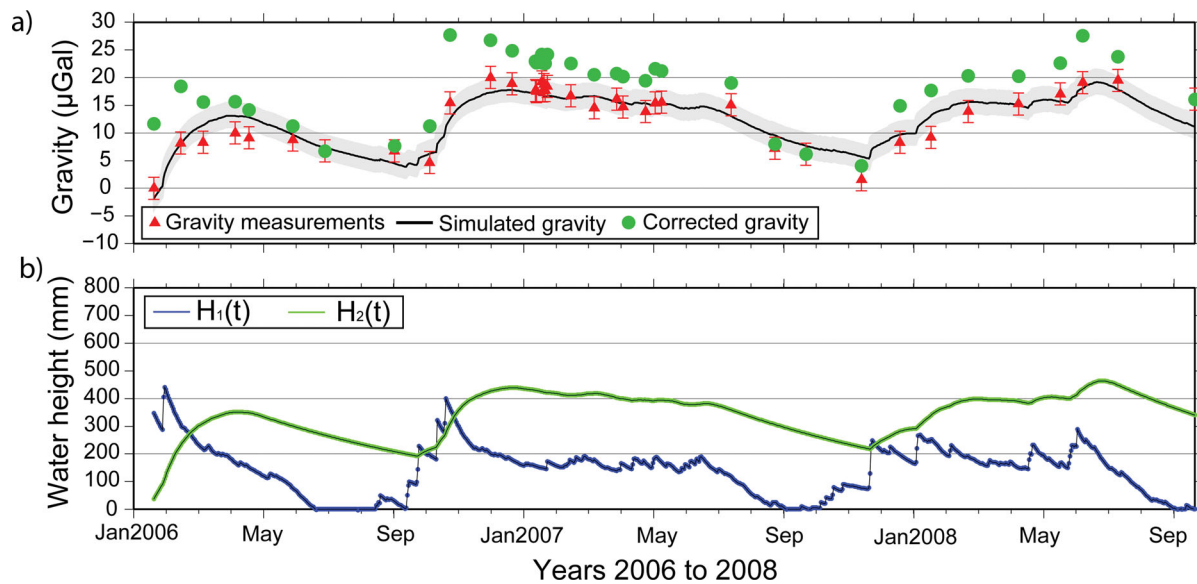


Figure 7. (a) Simulated gravity at SALV site using the two reservoir model (black line) and corrected gravity computed with $C_1 = 1$, and the estimated value of C_2 (green circle); (b) associated water height of the surface reservoir (blue line) and of the deep reservoir (green line).

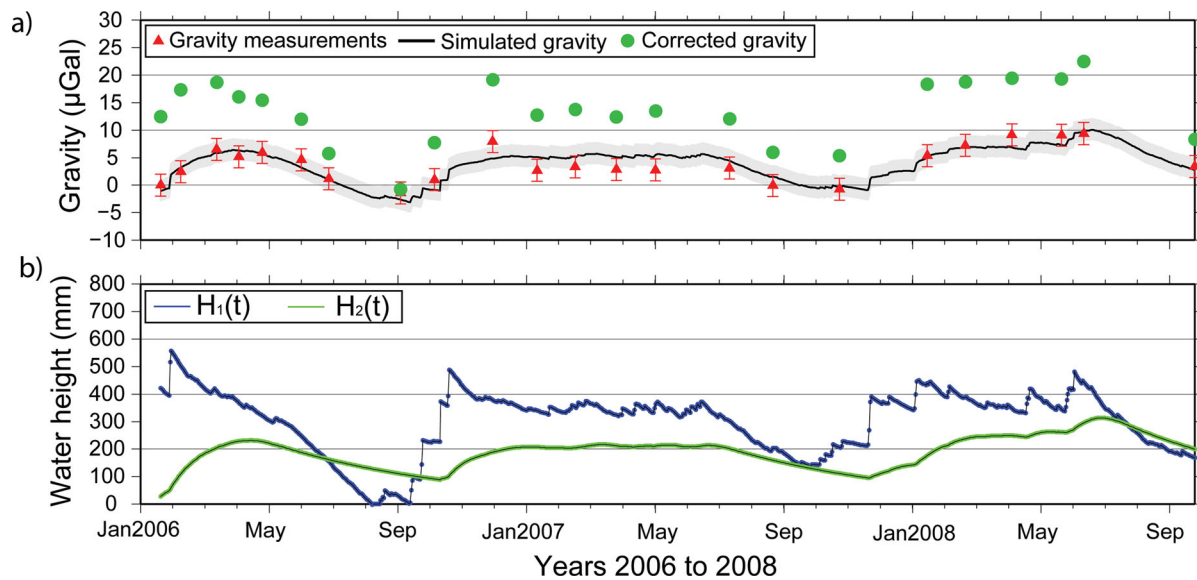


Figure 8. (a) Simulated gravity at CANA site using the two reservoir model (black line) and corrected gravity computed with $C_1 = 1$, and the estimated value of C_2 (green circle); (b) associated water height of the surface reservoir (blue line) and of the deep reservoir (green line).

assigned to 0.55, 0.65 and 0.75, respectively and are contained within the uncertainty of estimated parameters. Optimal values of all other estimated parameters remain close to those presented in Table 3.

6 INTERPRETATION AND DISCUSSION

6.1 Modelling local site effects

For the preferred reservoir model at each site, estimated values of C_1 (Table 3) for the surface reservoir are now compared to the forward computed site scaling factors C (Table 2). At CANA and SALV sites, estimated values of C_1 compare favourably with one another, being close to 0.2, and with the independently computed values of C for a layer of water at a depth of 1–2 m (Table 2).

Due to the similarity between the estimated values of C_1 and the forward modelled local site coefficients, it is tempting to associate the model surface reservoir with the hydrological functioning of the soil layer (~ 1 m depth) at SALV and CANA sites. At these two sites, the topography and building effects effectively mask out the effects of water storage changes in the upper meters of the karst on the observed gravity.

Within this scope, the estimated discharge constants of ~ 1 month for the surface reservoir at both sites (Table 2) may be associated with the time needed for rainwater to infiltrate to a depth below 1–2 m from the surface, depth at which local site effects become attenuated. Correlation between gravity variations and soil moisture content has been observed in several previous studies (e.g. Krause *et al.* 2009; Naujoks *et al.* 2010b) where the properties of the soil are globally homogeneous. In heterogeneous soils, as it often occurs in karst systems, distributed measurements seem mandatory in

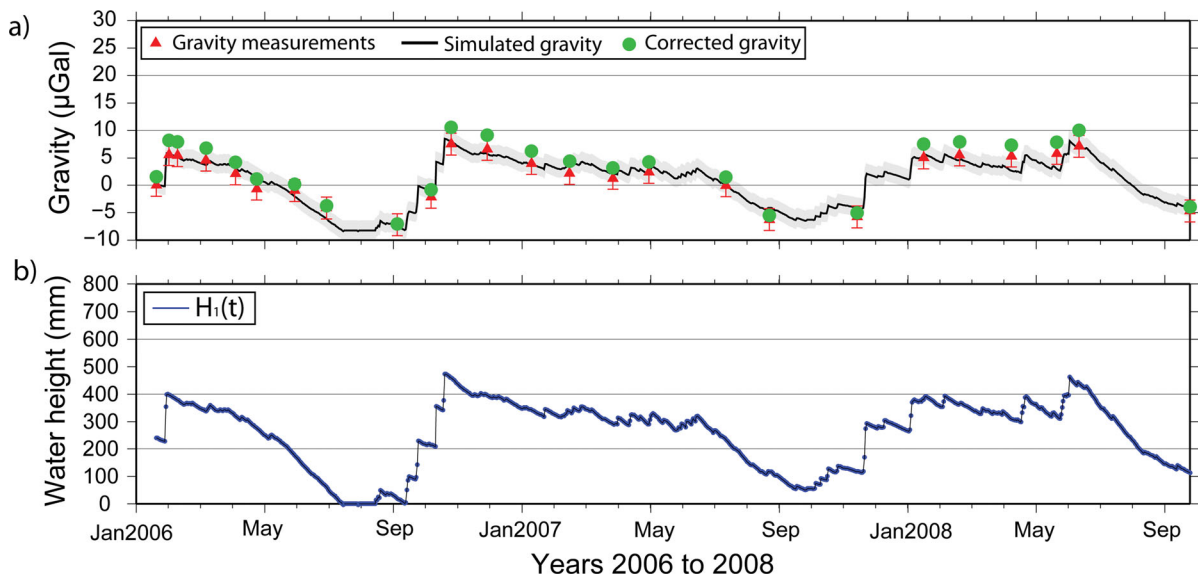


Figure 9. (a) Simulated gravity at BLAQ site using the single-reservoir model (black line) and corrected gravity computed with $C_1 = 1$ (green circle); (b) associated water height of the single reservoir (blue line).

order to obtain an average moisture value for the site (Creutzfeldt *et al.* 2010b). These *in situ* techniques (time or frequency domain reflectometry and capacity probes, for example) should yield insights on the saturation of the soil layer and should allow for a comparison with modelled water heights provided by gravity data inversion.

Gravity time-series modelling at CANA and SALV suggests that water storage changes are also associated to the second reservoir corresponding to a deeper horizon. Our modelling scheme assumes that water transfer with depth is strictly vertical. However, an estimated value of C_2 greater than unity could mean that the water level in the deep reservoir is influenced by lateral inflow, and not solely by vertical water transfer. Within this scope, the presence of lateral inflow within the deeper horizon at SALV may be invoked. At CANA, C_2 is close to 1, meaning that the full gravity attraction of the deep reservoir is felt, also indicating that the lateral flow budget of this reservoir is negligible. For these two sites, gravity measurements coupled with hydrological modelling provide a good insight of the time evolution of water storage change, bringing knowledge of local transfer properties. However, it must be noted that the deep reservoir of our model cannot be associated to a given depth.

At BLAQ site, where a single reservoir model accounts for storage changes seen by gravity, the C_1 coefficient is close to 0.8–0.9. Due to the small dimensions of the building at this site, the computed C_{total} coefficient is always larger than 0.7 as soon as water infiltrates below 1 m. This could explain why a single reservoir model accounts for water storage changes at BLAQ: rainwater has an immediate and significant influence on gravity, as the effects of water storage changes close to the surface are not masked out by the building.

The good agreement between the forward computed scaling coefficients representative of local site effects (Table 2) and the estimated ones (Table 3) suggests that the reservoir model formulation is a sound simplification of water storage change in the sites vicinity. Gravity changes may therefore be used to infer water storage changes using such models of vertical transfer. Inversion results provide an insight on the overall dynamics of the flow, which seems to correspond to a mostly vertical water transfer (where C_2 is equal to 1 like at BLAQ and CANA sites). However, some transient lateral

inflow component (at SALV site where C_2 is larger than unity) could be also invoked.

6.2 Use of ground-based gravity to monitor water storage changes

Ground-based gravity is one of the few means of monitoring local water storage changes in the vadose zone. Indeed, water storage change is usually obtained by a combination of measured and modelled input and output fluxes at basin scale. As such, a promising application of this gravity monitoring lies in its assimilation in hydrologic model calibration (Hasan *et al.* 2008; Creutzfeldt *et al.* 2010a; Naujoks *et al.* 2010a,b). Local site effects at every gravity measurement site must be evaluated and corrected for, so as to obtain gravity changes fully representative of water storage changes. As discussed, there are two means of evaluating local site effects: through a forward computation (Section 4) and through the use of reservoir models (Section 5). The forward computation necessitates a DEM of the site surroundings, the building dimensions and the knowledge of hydraulic properties of medium. Moreover, the depth at which water storage changes occur must be known, as a local site effect is strongly depth-dependent (Table 2). Other local factor such as impervious surfaces or the type of vegetation could be taken into account depending of the site characteristics.

If precipitation and evapotranspiration time-series are known, the adjustment of reservoir models using gravity data yields valuable information on flow dynamics and local site effects. When a two-reservoir model accounts for storage changes, the surface reservoir is plausibly representative of the first meters below the surface. The effect of water storage changes within these first meters may effectively be masked out by the building effects and the topography, as is the case at SALV and CANA sites. The deep model reservoir does not seem influenced by such factors (C_2 is close to or larger than unity at CANA and SALV). The sum of modelled water levels in the surface and deep reservoirs may therefore yield a more accurate approximation of water storage changes from gravity than using an infinite slab hypothesis (Fig. 6a). To summarize, the advantage of this approach is that no *a priori* knowledge of the underground

properties is needed. However, we acknowledge that the separation of the medium in two reservoirs is largely artificial even if we provided specific reasons to do so. Also, our model does not allow assigning a specific thickness to these reservoirs. It would be sound to apply our model reservoir approach on a well-instrumented site, including a superconducting gravimeter and a continuous geophysical and hydrological monitoring of water transfer in the vicinity of the site. This would lead to better understand the limits and the merits of the modelling presented here.

Once this validation done, a correction of ground-based gravity measurements from local site effect could be achieved. Indeed, our model only requires the knowledge of daily precipitation minus evapotranspiration. By adjusting the local reservoir model to the measured gravity, one can use the estimated coefficients to obtain a gravity time-series corrected for local site effects. To do so, we recall that local site effects are represented by the coefficient C_1 associated to the surface reservoir. Within this scope, one may augment the measured gravity by the “masked” signal from the surface reservoir, to obtain the corrected gravity time-series representative of total water storage changes:

$$g_{\text{cor}}(t) = g_{\text{mes}}(t) + 2\pi G\rho_w h_1(t)[1 - C_1], \quad (5)$$

where $h_1(t)$ and C_1 are the surface reservoir water level and scaling coefficient, respectively. The corrected gravity value is represented as green dots in Figs 7–9. This “corrected gravity” is the value that would be measured if the measurements were done in the same geometrical location but in an open field (no building) surrounded by a flat topography. This time-dependent correction shows that the gravity change due to local site effect can exceed measured values by 5–15 μGal , corresponding to 120–380 mm of water using the Bouguer’s slab formula. This finding confirms the remarks of Creutzfeldt *et al.* (2010b) on the importance of local site effects on time dependent gravity interpretations. This indicates that measured gravity must be corrected for these local effects for a more realistic interpretation in terms of water changes but also to compare the water storage behaviour between different sites. This remark is especially sound when open field gravity data with portable gravimeter are mixed with a gravimeter hosted in a large building with surrounding nonflat topography (e.g. Jacob *et al.* 2010). The models show that footprint of the building hosting the gravity measurement leads to a delay between the rainfall and the gravity maximum. When topography around the site is not strictly flat, the maximum of the measured gravity due to a rainfall can be modified. It decreases by a factor up to 4 in this study for the site CANA. Keeping in mind that corrections always have uncertainty, the impact of topography and building should be minimized. It is then important for future studies to take into account these effects and to choose a site where building is small and topography as flat as possible.

7 CONCLUSION

Ground-based gravity measurements provide valuable data for hydrogeological studies. However, we show that an interpretation of gravity change using an infinite Bouguer slab of groundwater is only possible in ideal sites (no topography, no building, and horizontally homogeneous water transfer properties). Buildings and topography strongly alter the gravimetric signal and may mask most of the attraction of an infinite slab of water immediately after rainfall. A simple two-reservoir model allows the separation between topographic and building umbrella effects and the effective groundwater transfer properties. The modelling of the gravity measurements using such

a model on the Larzac plateau also reveals a spatial heterogeneity of transfer properties from one site to another. For example, characteristic transfer times associated to deep transfer may vary from five months to about ten months. We show that coupling gravity data time-series with hydrologic modelling is a useful method to determine both averaged transfer properties and local site effects. It would be sound to use and test this methodology to process the near continuous gravity signal recorded by superconducting gravimeters. Such studies should provide interesting insights as to the best-suited measurement configurations for future gravity studies.

ACKNOWLEDGMENTS

We thank Nicolas Le Moigne who provided a decisive help in data acquisition using FG5 gravimeter. This project is part of ‘Hydro-karst Géophysique et Géodésie’ (HydroG2) supported by the ‘Agence Nationale de la Recherche’ (ANR). Some climatic and hydrologic data were provided by the Parc Régional des Grands Causses and Météo France. We thank B. Creutzfeldt, an anonymous reviewer and the editor for their constructive comments.

REFERENCES

- Allen, G.A., Pereira, L.S., Raes, D. & Smith, M., 1998. *Crop Evapotranspiration – Guidelines for Computing Crop Water Requirements*, Rome, FAO – Food and Agriculture Organization of the United Nations, Rome.
- Boy, J.P., Hinderer, J. & Gegout, P., 1998. Global atmospheric loading and gravity, *Phys. Earth planet. Inter.*, **109**, 161–177.
- Creutzfeldt, B., Guntner, A., Klugel, T. & Wziontek, H., 2008. Simulating the influence of water storage changes on the superconducting gravimeter of the Geodetic Observatory Wettzell, Germany, *Geophysics*, **73**(6), WA95–WA104.
- Creutzfeldt, B., Guntner, A., Vorogushyn, S. & Merz, B., 2010a. The benefits of gravimeter observations for modelling water storage changes at the field scale, *Hydrol. Earth Sys. Sci.*, **14**(9), 1715–1730.
- Creutzfeldt, B., Guntner, A., Wziontek, H. & Merz, B., 2010b. Reducing local hydrology from high-precision gravity measurements: a lysimeter-based approach, *Geophys. J. Int.*, **183**, 178–187.
- Creutzfeldt, B., Guntner, A., Thoss, H., Merz, B. & Wziontek, H., 2010c. Measuring the effect of local water storage changes on in situ gravity observations: case study of the Geodetic Observatory Wettzell, Germany, *Water Resour. Res.*, **46**, W08531, doi:10.1029/2009WR008359.
- Fleury, P., Plagnes, V. & Bakalowicz, M., 2007. Modelling of the functioning of karst aquifers with a reservoir model: application to Fontaine de Vaucluse (South of France), *J. Hydrol.*, **345**(1–2), 38–49.
- Harnisch, G. & Harnisch, M., 2006. Hydrological influences in long gravimetric data series, *J. Geodyn.*, **41**, 276–287.
- Hasan, S., Troch, P.A., Bogaart, P.W. & Kroner, C., 2008. Evaluating catchment-scale hydrological modeling by means of terrestrial gravity observations, *Water Resour. Res.*, **44**, W08416, doi:10.1029/2007WR006321.
- Hokkanen, T., Korhonen, K. & Virtanen, H., 2006. Hydrogeological effects on superconducting gravimeter measurements at Metsähovi in Finland, *J. Environ. Eng. Geophys.*, **11**(4), 261–267.
- Jacob, T., 2009. Apport de la gravimétrie et de l’inclinométrie à l’hydrogéologie karstique, in *Geosciences Montpellier*, pp. 283, Université des Sciences et Technologies, Montpellier.
- Jacob, T. *et al.*, 2008. Absolute gravity monitoring of water storage variation in a karst aquifer on the Larzac plateau (Southern France), *J. Hydrol.*, **359**(1–2)doi:10.1016/j.jhydrol.2008.1006.1020.
- Jacob, T., Bayer, R., Chery, J. & Le Moigne, N., 2010. Time lapse micro-gravity surveys reveal water storage heterogeneity of a karst aquifer, *J. geophys. Res.*, **115**, B06402, doi:10.1029/2009JB006616.
- Krause, P., Naujoks, M., Fink, M. & Kroner, C., 2009. The impact of soil moisture changes on gravity residuals obtained with a superconducting gravimeter, *J. Hydrol.*, **373**, 151–163.

- Lambert, A. & Beaumont, C., 1977. Nano variations in gravity due to seasonal groundwater movements: implications for the gravitational detection of tectonic movements, *J. geophys. Res.*, **82**, 297–306.
- Lampitelli, C. & Francis, O., 2010. Hydrological effects on gravity and correlations between gravitational variations and level of the Alzette River at the station of Walferdange, Luxembourg, *J. Geodyn.*, **49**(1), 31–38.
- Longuevergne, L., Florsch, N., Boudin, F., Oudin, L. & Camerlynck, C., 2009. Tilt and strain deformation induced by hydrologically active natural fractures: application to the tiltmeters installed in Sainte-Croix-aux-Mines observatory (France), *Geophys. J. Int.*, **178**, doi:10.1111/j.1365-246X.2009.04197.x.
- Maillet, E., 1905. *Essais d'hydraulique souterraine et fluviale*, Hermann, Paris.
- Mäkinen, J. & Tattari, S., 1988. Soil moisture and groundwater: two sources of gravity variations, *Bull. d'Inf. Marées Terr.*, **63**, 103–110.
- Naujoks, M., Kroner, C., Weise, A., Jahr, T., Krause, P. & Eisner, S., 2010a. Evaluating local hydrological modelling by temporal gravity observations and gravimetric three-dimensional model, *Geophys. J. Int.*, **182**, 233–249.
- Naujoks, M., Weise, A., Kroner, C. & Jahr, T., 2010b. Detection of small hydrological variations in gravity by repeated observations with relative gravimeters, *J. Geod.*, **82**(9), 543–553.
- Niebauer, T.M., Sasagawa, G.S., Faller, J.E., Hilt, R. & Klotz, F., 1995. A new generation of absolute gravimeters, *Metrologia*, **32**, 159–180.
- Ricard, J. & Bakalowicz, M., 1996. Connaissance, aménagement et protection des ressources en eau du Larzac septentrional, Aveyron (France). Report R38953, BRGM, Orléans.
- Rodell, M. *et al.*, 2004. The global land data assimilation system, *Bull. Am. Meteorol. Soc.*, **85**(3)doi:10.1175/BAMS-1185-1173-1381.
- Seibert, J., 2005. *HBV Light Version 2, User's Manual*, Uppsala University, Uppsala.
- Van Camp, M., Vanclooster, M., Crommen, O., Petermans, T., Verbeeck, K., Meurers, B., van Dam, T. & Dassargues, A., 2006. Hydrogeological investigations at the Membach station, Belgium, and application to correct long periodic gravity variations, *J. geophys. Res.*, **111**, B10403, doi:10.1029/2006JB004405.
- Wagner, T., Gupta, H.V. & Sorooshian, S., 2004. Stochastic formulation of a conceptual hydrological model, *Hydrology*, **1**, 398–405.
- Zhang, Z., Chen, X., Ghadouani, A. & Peng, S., 2011. Modelling hydrological processes influenced by soil, rock and vegetation in a small karst basin of southwest China, *Hydrol. Process.*, **25**, 2456–2470.